Analysis and Design of a Small Size Rotary Ultrasonic Motor

Jong-Seok Rho and Hyun-Kyo Jung
School of Electrical Engineering
Seoul National University University
San 56-1, Sillim-dong, Gwanak-gu, Seoul, 151-742
Korea
http://elecmech.snu.ac.kr/

Abstract: - Up to the present time, the analysis and design of the USM have been almost always performed using rough analytic methods or using commercial analysis tools or using the trial and error method without considering the USM's contact mechanisms. As a result, it was impossible to achieve an exact and efficient analysis and design of the USM. In order to address this problem, we propose the analysis and design methodology of the 8.5[mm] outer diameter RUSM using a numerical method that is the Three Dimensional Finite Element Method (3D-FEM) for a steady state analysis and the Three Dimensional Finite Difference Method (3D-FDM) for a transient analysis. And these numerical methods are combined with an analytic method. Among the analytic method important one is the Cutting Method (CM), which we proposed and named in this paper. Also, this methodology takes the contact mechanism into consideration in linear operation. The important one is that it can be applied to many other kinds of USM which use the same working mechanisms.

In addition, four kind of comb-tooth structures of the proposed RUSM is prototyped in this research. Finally, the relation between the speed of motor and the tooth number is revealed at the first time. It has the meaning because there is almost nothing at all about the tooth design method. Also, by the prototyped RUSM, the proposed analysis and design methodology is validated by comparing its outcomes with the experimental data.

Key-Words: - Actuator, FEM, FDM, rotary motor, piezoelectric, small size, ultrasonic motor, 8.5[mm] diameter.

1 Introduction

The numerous merits associated with the USM have prompted many researchers to perform widespread studies over several decades [1]-[7]. However, precise and efficient analysis and design are impossible because the USM uses very complicated dynamic mechanisms, such as electromechanical coupling and mechanical friction. But, the analysis and design of the USM have been almost always performed using rough analytic methods or using commercial analysis tools or using the trial and error methods without considering the USM's contact mechanisms up to the present time [1]-[7]. As a result, it was impossible to achieve an exact and efficient analysis and design of the USM. In order to address this problem, we propose the analysis and design methodology of the 8.5[mm] outer diameter RUSM using a numerical method that is the 3D-FEM for a steady state analysis and the 3D-FDM for a transient analysis. And these numerical methods are combined with an analytic method. Among the analytic method important one is the Cutting Method (CM), which we proposed and named in this paper. Also, the proposed methodology sheds light on a complex contact mechanism in linear operation. The important one is that it can be applied to many other kinds of USM which use the same working mechanisms.

In addition, four kind of comb-tooth structures of the proposed RUSM is prototyped in this research. Finally, the relation between the speed of motor and the tooth number is revealed at the first time. It has the meaning because there is almost nothing at all about the tooth design method. Also, by the prototyped RUSM, the proposed analysis and design methodology is validated by comparing its outcomes with the experimental data.

2 Characteristic Analysis and Design of a RUSM

2.1 Traveling wave analysis and design of a piezoelectric ceramic by analytic method

The first stage for the design of a RUSM is the design of a piezoelectric ceramic using analytic method. In this research, we proposed a geometric for the piezoelectric ceramic as shown in Fig.1 for a 8.5[mm] outer diameter RUSM taking the size and effective generation of traveling wave into consideration. At

first, the generation of a traveling wave for this model is verified by using an analytic method.

If the amplitude of two electrical sources is the same then the summation of waves at each piezoelectric ceramic is expressed by :

$$\sum_{i=0}^{3} A\sin\{wt-k(x+a\times i)+\varphi\times i\} + A\sin\{wt+k(x+a\times i)+\varphi\times i\} \quad (1)$$

where,
A : amplitude of the wave
k : the wave number k.

As shown in Fig.1, the space difference between two piezoelectric ceramics a follows :

$$a=\pi/2 \quad (2)$$

We designed the piezoelectric ceramic pattern as shown in Fig.1 for the generation of 3λ. Hence the wave length λ should be 2π/3. Using this values and from (3), we derived the wave length λ, as follows :

$$a=\frac{2\pi}{k}\frac{(n-m)}{4}=\frac{\lambda(n-m)}{4} \quad (3)$$

hence,

$$\lambda=\frac{4a}{(n-m)}=\frac{2\pi}{3}. \quad (4)$$

Therefore, *(n-m)* should be 3. Using this value and from (3), we derived the wave number k, as follows :

$$k=\frac{2\pi}{a}\frac{(n-m)}{4}=3. \quad (5)$$

By applying (2)-(5) into (1), (1) is summarized into :

$$16A\sin(wt-kx) \quad (6)$$

From this result, it is verified at first by the analytic method that the proposed model generates a traveling wave and can be used for the vibrator of a RUSM.

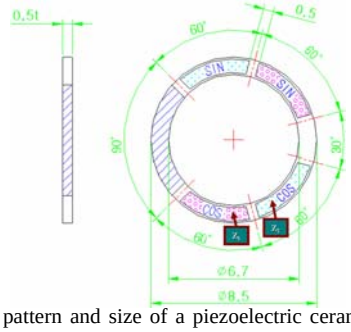

Fig.1. Proposed pattern and size of a piezoelectric ceramic for a 9[mm] outer diameter RUSM

2.2 Impedance analysis and design of a vibrator for a RUSM using an analytic method

The second design stage is the rough analysis and design of the vibrator for a RUSM considering the resonance frequency of a vibrator for a RUSM by an analytic method.

The reason of rough analysis and design of vibrator using analytic method prior to the FEM analysis is to reduce the calculating time of the FEM. The calculation for finding the resonance frequency value using the FEM takes much time because it needs frequency sweep. Also, this is because a designer can roughly design the vibrator considering the restricting design components, such as the size and operating frequency, and so on in this step. Hence, the rough finding of a resonance frequency prior to the calculation of the FEM is essential. The frequency f_n for the n-th mode wave is expressed by [1],[2] :

$$f_n=\frac{\pi n^2}{2l^2}\sqrt{\frac{EI}{\rho S}} \quad (7)$$

where,
f_n : frequency for n-th mode wave
n : vibration mode number
l : length of a ring
E : young's modulus
I : the second moment of area
ρ : density
S : ring's cross-sectional area

To determine the value of variables in (7), the cross section of a vibrator for a RUSM is assumed as shown in Fig. 2(a). The ceramic and the metal have different Young's modulus that the cross-section should be transformed into an equivalent cross-section as shown in Fig.2(b) [2]. The transformed width b_2 shown in

Fig.2 can be calculated by the relationship between the width and the young's modulus, as follows :

$$\frac{b_2}{b_3} = \frac{c_{11}}{E_m} \tag{8}$$

where,
c_{11} : Young's modulus of the piezoelectric ceramic to the 1-1 direction
E_m : young's modulus of the metal.

The vibration mode number n subjects to :

$$n = 2m \tag{9}$$

where,
m : number of wave cycles present on the ring (correspond to the number of pole pairs).

The length of a ring l is expressed by :

$$l = \pi \frac{(D_o + D_i)}{2} \tag{10}$$

where,
D_o : outer diameter
D_i : inner diameter.

The cross-sectional area S is given by :

$$S = b_1 h_1 + b_2 h_2 \tag{11}$$

The second moment of area I is given by :

$$I = \frac{1}{3} b_2 \left(h_N^3 + h_M^3\right) + b_1 h_1 \left(h_M - \frac{h_1}{2}\right)^2 + \frac{b_1 h_1^3}{12} \tag{12}$$

in which, the neutral plane's height h_N and the height h_M are expressed by :

$$h_N = \frac{b_1 h_1^2 + b_2 h_2^2}{2\left(b_1 h_1 + b_2 h_2\right)} \tag{13}$$

$$h_M = h_2 - h_N \tag{14}$$

By using (8)-(14) and values shown in Table 1, the roughly calculated 6-th mode resonance frequency of a designed vibrator for a 8.5[mm] outer diameter RUSM is 208,850 [Hz]. This calculated resonance frequency by analytic method shows large difference with the experimental result 248,125 [Hz]. Hence, a 3D-FEM is needed for the exact and efficient impedance analysis of a RUSM. But, this analytic result gives designer the rough resonant frequency value at first easily and quickly. Therefore, we don't need to sweep a large frequency section but only sweep near 208,850 [kHz] in the FEM calculation. As a result, the calculating time of the FEM could be saved so much. Also, we completed the rough design of a vibrator for a 8.5[mm] outer diameter RUSM considering the restricting design components, such as the size and operating frequency, and so on.

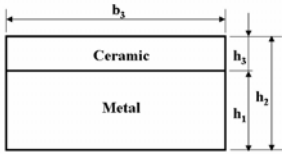

(a) Cross-section of a vibrator for a RUSM

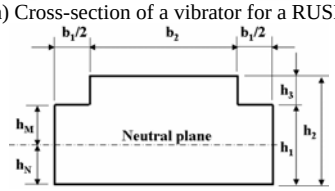

(a) Transformed cross-section of a vibrator for a RUSM

Fig.2. Cross-section and transformed cross-section of a vibrator for a RUSM.

Table 1. Value of variables for the analysis and design of an impedance of a vibrator using an analytic method

Vriables	Value
Number of a wave cycle (m)	3
Vibration mode number (n-th mode)	6
Outer diameter (D_o)	8.5E-3 [m]
Inner diameter (D_i)	6.7E-3 [m]
Length of a vibrator (l)	23.88E-3 [m]
Width of a vibrator (b_3)	0.9E-3 [m]
Transformed width of a piezoelectric ceramic (b_2)	1.06E-3 [m]
Height of a metal (h_1)	1.5E-3 [m]
Height of a piezoelectric ceramic (h_3)	0.5E-3 [m]
Height of a neutral plane (h_N)	1.03E-3 [m]
Cross-section area (S)	1.88E-6 [m^2]
The second moment of area (I)	0.65E-12 [m^2]
Density (ρ)	8780 [kg/m^3]
Young's modulus of the piezoelectric ceramic to the 1-1 direction (c_{11})	1.33E+11 [N/m^2]
Young's modulus of the metal (E_m)	1.12E+11 [N/m^2]

2.3 Impedance/ mode analysis and design of the vibrator for a RUSM using 3D-FEM

To find out the resonance frequency, which generates the desired mode, the impedance and the mode are analyzed by using the 3D-FEM at this design stage. To calculate the impedance of a RUSM, which is shown

in Fig.3, the impedance (77) has to be modified due to the parallel electrodes of the RUSM, as follows :

$$\frac{1}{Z_{tot}(w)} = \sum_{i=1}^{n} \frac{1}{Z_i(w)} = \frac{Z_2 Z_3 ... Z_{n-1} Z_n + Z_1 Z_3 ... Z_{n-1} Z_n + ... + Z_1 Z_2 ... Z_{n-2} Z_{n-1}}{Z_1 Z_2 ... Z_{n-1} Z_n} \quad (15)$$

where,
Z_{tot} : total impedance of the RUSM
Z_i : impedance at i-th input part
n : total number of paralleled input part (in this case n=2).

Hence, the impedance of the RUSM is expressed by :

$$Z_{tot}(w) = \frac{\prod_{k=1}^{n} Z_k}{\sum_{i=1}^{n} \prod_{j=1, j\neq i}^{n} Z_j} \quad (16)$$

where,
$\prod_{j=1, j\neq i}^{n} Z_j$: accumulated multiplication from j is 1 to n except when j=i.

Fig.3 compares the impedance between the simulation and the experiment. The simulation result is obtained by the 3-D FEM and (16), and experimental data by the impedance analyzer. As shown in Fig.3, the data of the simulation is almost in agreement with the experimental data. This agreement proves that the 3-D FEM routine used in this research is correct. The calculated resonance frequency value, which generate the desired mode properly, is 246,200[Hz] and the experimental one is 248,125[Hz]. Fig.4 shows the calculated result of a 6-th mode wave at the calculated resonance frequency 246,200[Hz] with 14.14[V_{rms}] input voltage. In briefly, the vibrator of a 8.5[mm] outer diameter RUSM is analyzed and designed considering the resonance frequency, the mode, the size, and so on using a 3D-FEM at this design stage.

In this research, four kinds of teeth are made varying the number of tooth, such as 12, 16, 18, and 22. This is because to find out the relation between the tooth number and the speed of motor, also to verify the Cutting Method (CM) theory. These related ones will be explained more precisely at section 2.5. The metal part of the vibrator is a phosphor-bronze. Since, the phosphor bronze has the good properties for the vibrator of a RUSM, such as superior anti-abrasion and nearly uniform young's modulus insensitivity to temperature change.

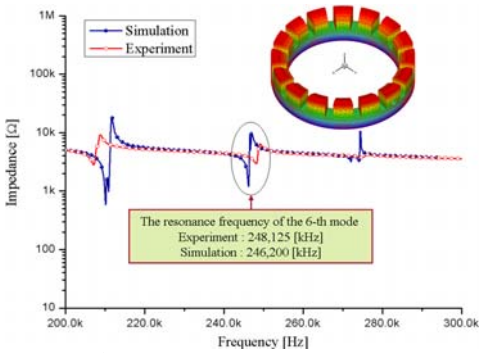

Fig.3. Impedances of the 8.5[mm] outer diameter RUSM obtained from the simulation and the experimental

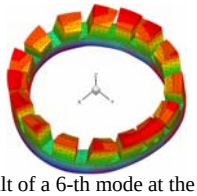

Fig.4. Calculated result of a 6-th mode at the resonance frequency 246,200[Hz] with 14.14[V_{rms}] input voltage.

2.4 Analysis of an elliptical motion using a 3D-FEM and an analytic method

In this research, we assumed that the rotor and the stator are rigid body that they dose not mechanically deform. This is because we take the stator into account only when ideal no mechanical load is applied to. And, because the applied mechanical load to the rotor and the stator is so small that the deformation of them is ignorable. To simplify the problems, we also assumed that the contact only occurs at the three peak points to normal direction when ideal no mechanical load is applied to. One of the important assumptions is that only three peak points to normal direction have to be considered although there are over three wave peaks. The reason of only considering three points is that the point number for sustain some body is only three points although there are over three wave peaks. Therefore, the elliptical displacement is calculated at the three peak teeth as shown in Fig.5. The peak tooth is the one of which normal displacement to the +z-direction is maximum.

The displacement to the x-, y-, and z-direction is simulated at contacting three peak nodes using the 3D-FEM. The elliptical displacement can be drawn according to divisional steps at one contacting point by :

$$x_i = |x_{com}| \times \sin\left[\frac{2\pi}{n} \times i + rad(x_{com})\right] \quad (17)$$

$$y_i = |y_{com}| \times \sin\left[\frac{2\pi}{n} \times i + rad(y_{com})\right] \quad (18)$$

$$z_i = |z_{com}| \times \sin\left[\frac{2\pi}{n} \times i + rad(z_{com})\right] \quad (19)$$

where,
x_i, y_i, z_i : value of x-, y-, z-directional displacement at the i-th divisional step of an elliptical displacement
x_{com} : complex of a displacement to x-direction
y_{com} : complex of a displacement to y-direction
z_{com} : complex of a displacement to z-direction
n : total divided number of an elliptical motion
i : from 0 to n
rad(k) : radian of a complex k.

The rotary speed of a RUSM is determined by the velocities of elliptical displacements, especially by the tangential ones about the circle of a motor. Hence, to simulate the RPM (Revolution Per Minute) of a RUSM, the original coordinate axis of each elliptical motion must be transformed to a new coordinate axis which is a rotated one to the tangential direction of a circle, as shown in Fig.6.

The general formulation of a transformed node value by coordinate axis's rotation is (20) and (21). Therefore, (22)-(24) are derived for the calculation of a transformed elliptical motion, of which coordinate axis is a rotated one to the tangential direction of a circle.

$$X' = \cos(\theta)X + \sin(\theta)Y \quad (20)$$

$$Y' = -\sin(\theta)X + \cos(\theta)Y \quad (21)$$

where,
X, Y : X, Y values about an original coordinate axis
$X`$, $Y`$: transformed X, Y values about a rotated coordinate axis.

Hence,

$$x_i` = \sin(\theta)x_i - \cos(\theta)y_i \quad (22)$$

$$y_i` = \cos(\theta)x_i + \sin(\theta)y_i \quad (23)$$

$$z_i = z_i \quad (24)$$

where,
x_i, y_i, z_i : x, y, z values, which are calculated by means of (17)-(19)
$x_i`$, $y_i`$: transformed x_i, y_i values about a rotated coordinate axis to the tangential direction of a circle, at the i-th divisional step of an elliptical displacement.

Fig.7 displays the elliptical motion, which was calculated with (22)-(24), for the suggested 6-th mode RUSM at three contacting points when a 14.14[V_{rms}]/246,200[Hz] electrical input source was applied to the vibrator. From this result, the possibility of proper motion of the RUSM is identified at the primary stage by checking some factors. Important checking factors and the design solution when it dose not satisfy the checking factors are summarized, as follow :

1) Amplitude of the displacement : more than 5E-7 meters of displaced amplitude is better for proper operation. If not, then a design modification is needed for a vibrator to amplify the displacement, such as increasing the teeth height, or raising the maximum voltage, or decreasing the thickness of piezoelectric ceramic, and so on.
2) Shape of the elliptical motion : the horizontal direction's displacement component of elliptical motion has an effect on the velocity of the motor and normal direction's displacement component on the torque of the motor [1]-[5]. If the elliptical motion is not proper, such as too sharp that almost line shape of elliptical motion is generated then design modification is needed for a vibrator to form the proper elliptical motion by increasing or decreasing the horizontal or normal direction's displacement. The analysis and design method, which related the shape of an elliptical motion, will be and have to be dealt with precisely at the next design stage.
3) Rotation's direction of the elliptical motion : rotation's direction of the elliptical motion at all sampling points must be the same for efficient operation of a RUSM. If not then they cancel out each other so that the motor does not operate or the performance of motor is decreased. Therefore, a modification of design is needed such as cutting some part of the teeth, in which the elliptical motion to the inverse direction is generated, or so on.
Also, the clockwise or the counterclockwise rotation of the elliptical motion must be checked by changing two electrical input sources using the 3D-FEM. This is because the rotating direction of a RUSM is determined by that of the elliptical motion.

The elliptical motions of the proposed RUSM are generated with satisfying the above three check factors

at all three contacting points as shown in Fig.11. From those results, it is verified, at the primary stage, that the designed RUSM could operate effectively.

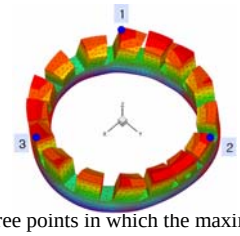

Fig.5. Contacting three points in which the maximum displacement is generated to the +z-direction.

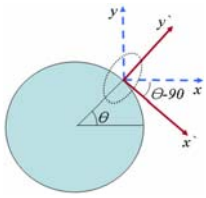

Fig.6. Rotation of the original coordinate axis to the tangential direction of a circle.

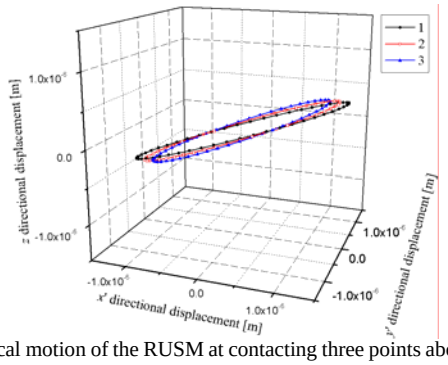

(a) Elliptical motion of the RUSM at contacting three points about $x`$, $y`$, z coordinate aix

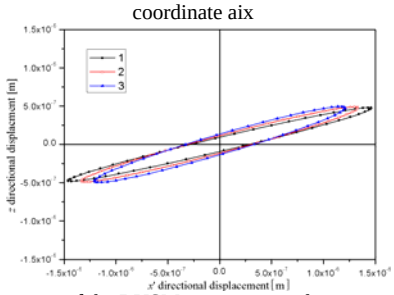

(b) Elliptical motion of the RUSM at contacting three points about the $x`$, z coordinate aix

Fig.7. Elliptical motion of the RUSM at three contacting points.

2.5 Characteristic analysis and design of the RUSM using a 3D-FEM combined with an analytic method.

Motor characteristics are calculated as follow steps.

1) Analysis of an elliptical motion using the proposed Cuting Method (CM).

We propose in this research the CM for the analysis of the USM's velocity when ideal no mechanical load is applied to. We named proposed method the CM. This is because the velocity of USM is calculated by cutting an elliptical motion taking the contacting time into the consideration. If an USM uses j number of teeth in the 1λ section as shown in Fig.8 (a) then the contact duration of a peak elliptical motion is only the upper part in the cut ones into $1/j$, as shown in Fig.8 (b). The rotary speed of a RUSM is determined by the velocity, of which direction is to the tangential ones about the circle of a motor, of elliptical displacements. Hence, to calculate the USM'S velocity, the tangential velocity to the transformed horizontal $x`$ direction taking the contact duration $(x`)_{contact}$ have to be calculated. And, it is derived by (25) considering the upper part shown in Fig.8.

$$(v_{x`})_{contact} = \frac{\Delta x`}{contacting\ time} = \frac{\Delta x`}{\left(\frac{DN}{f \times n}\right)} \qquad (25)$$

where,

$(v_{x`})_{contact}$ : tangential velocity to the transformed horizontal $x`$ direction taking the contact duration

$\Delta x`$ : displaced amount to the transformed $x`$ direction as shown in Fig.8

DN : divided number of an elliptical motion during the contact duration

f : frequency

n : total divided number of an elliptical motion

The important one is that we propose the $\Delta x`$ for the calculation of the USM's velocity. The $\Delta x`$ must not be confused with $\Delta x`_2$ as shown in Fig.8. This is because finally displaced total amount to $x`$ direction is $\Delta x`$ not $\Delta x`_2$ during the contact duration. Hence, the important one is when designer checks the shape of an elliptical motion, as mentioned in section 2.4 at the second checking factor part, a designer must consider the $\Delta x`$ not the $\Delta x`_2$.

According to the proposed CM, the speed of a USM can be increased by increasing the number of tooth. This is because the cutting number is increased in proportional to the increase of teeth number. And, the increase of cutting number induces the reduction of the contacting time more largely than the decrease of the $\Delta x`$. Hence, this phenomenon causes the rise of the motor speed from Fig. 8 and (25). This theory and result are verified from the experiment data as shown

in Table 2. Also, this experiment data validates the reasonableness of the CM. Although, twenty-two number of comb-tooth structure is the fastest one, we will deal with sixteen number of comb-tooth structure from now. This is because over sixteen is hard to make and expensive.

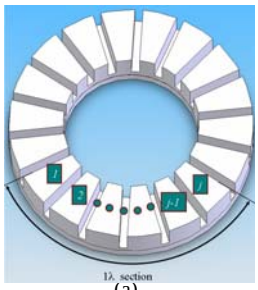

(a)

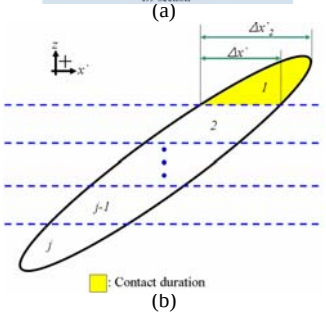

(b)

Fig.8. Proposed Cutting Method taking the contact mechanism into the consideration.

Table 2. The relation between the number of tooth and the speed of motor

Number of tooth	Speed of motor
12	565[rpm]
16	780[rpm]
18	892 [rpm]
22	983 [rpm]

2) Analysis of the motor performance.
The relation between the velocity to the tangential direction at a circle v[m/s] and the rotating number of circle per one second f [Hz] is expressed by (26)

$$f = v/(2\pi \times r) \tag{26}$$

where,
r : radius from the sampling point to the center of a circle [m]
v : velocity to the tangential direction at a circle[m/s].

Hence, (27) is proposed to simulate the rotating number of the motor per one second f_M [Hz].

$$f_M = \frac{(v_{x`})_{contact}}{2\pi \times r} \tag{27}$$

where,
r : Radius from the sampled node to the center of a motor [m]

As mentioned in section 2.4, we sampled three peak points, which are the largest ones to the normal z direction. Hence, the rotary speed of a RUSM at k-th point is expressed by :

$$(RPM_M)_k = (f_M)_k \times 60 \tag{28}$$

where,
RPM_M : Revolution Per Minute of the Motor[rpm]
k : k-th sampled peak point.

Finally, the calculated $(RPM_M)_k$, k is from 1 to 3, values are averaged to calculated the USM's final velocity RPM_M, as follows :

$$RPM_M = \frac{\sum_{k=1}^{3}(RPM_M)_k}{3} \tag{29}$$

The torque of a RUSM T is derived using the friction force F_f, as follows:

$$T = -|F_f| \times r_{eff} = -sign[f_M] \times |\mu_d \times F_{mpf}| \times r_{eff} \tag{30}$$

which subjects to,
$f_M > 0 \quad \Rightarrow \quad sign[f_M] = +1$
$f_M < 0 \quad \Rightarrow \quad sign[f_M] = -1$

where,
F_f : friction force
r_{eff} : effective radius of the contacting teeth from the center of a motor
$_d$: dynamic coefficient of friction
F_{mpf} : mechanical perpendicular force which is the sum of the mechanical pressing force and the weight of the rotor.

The mechanical output power of a motor P_{out} is expressed by:

$$P_{out} = w_M \times T = \frac{2\pi}{60} RPM_M \times T \tag{31}$$

where,
w_M : angular velocity of a motor [rad/s].

Thus, the efficiency of a motor about input electrical power P_{in} is given by:

$$\eta = \frac{P_{out}}{P_{in}} \quad . \tag{32}$$

Fig.9 shows the experiment result of the Torque-Speed and the linearly approximated experiment data to calculate the ideal no mechanical load speed. The linearly approximated equation of experiment data is expressed by :

$$w = -363.85T + 805.05 \tag{33}$$

We calculated the ideal no mechanical load speed by (33) using experiment result, and the result is 805.05[rpm]. Hence, we compared the simulation result, which was calculated by the suggested 3D-FEM combined with an analytic method, with the experimental ideal no mechanical load speed. The simulated speed is 818 [rpm] and this shows the reasonable agreement with the experiment result 805.05 [rpm], within 1.6% error. This result verified that the proposed characteristic analysis and design methodology is validates.

Fig. 10 shows the transient analysis result of the proposed RUSM using the 3D FDM. As shown in Fig.10, when the speed is arrived to the steady state, the speed of motor is 816 [rpm]. This result also validated the proposed characteristic analysis and design methodology. The important one in transient analysis result is that only it takes under 1 [msec] to arrive the steady state.

Fig.11 indicates the speed and the efficiency of the proposed RUSM about the varying torque of motor when 14.14[V_{rms}] is applied to. The main characteristics of this motor are tabulated in Table 3.

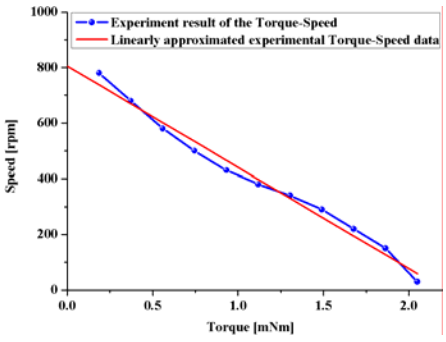

Fig.9. Experiment result of the Torque-speed and the linearly approximated experiment data when 14.14[V_{rms}] is applied to.

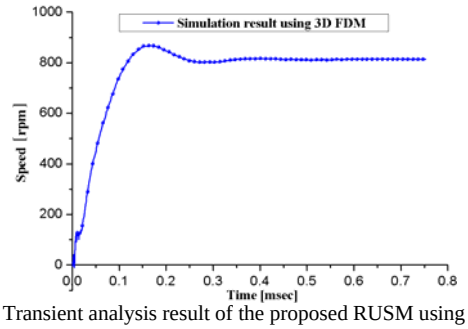

Fig.10. Transient analysis result of the proposed RUSM using the 3D FDM.

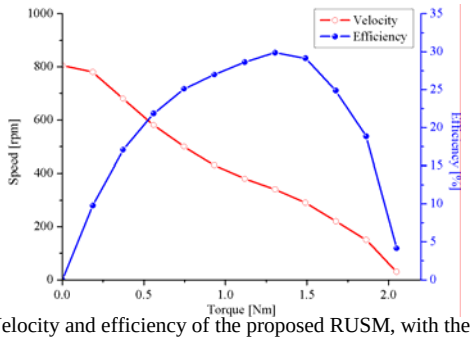

Fig.11. Velocity and efficiency of the proposed RUSM, with the varying torque of motor, when the electrical input source 14.14[V_{rms}]/248,125[Hz] was applied to.

Table 3. Main characteristics of the B_{14} RUSM.

Specification	Value
Operating frequency	249.1 [kHz]
Rating input voltage	14.14 [V_{rms}]
Maximum speed	1240 [rpm]
Maximum torque	1.05 [mNm]
Maximum output	0.34 [W]
Maximum efficiency	36.98 [%]

3 Prototype of the B_{14} RUSM

Fig.12 shows the bottom side of the prototyped vibrator that displays the electrode pattern of the prototyped piezoelectric ceramic of the 8.5[mm] outer diameter RUSM. The piezoelectric ceramic is made from the Dong-Il and the comb-tooth structure is made from the phosphor bronze. Fig.13 indicates the prototyped comb-tooth structures. As mentioned in section 2.4, we prototyped four kinds of comb-tooth structures varying the number of tooth. The reason of that is to find out the relation between the number of tooth and the speed of motor. Another one reason is to verify the proposed CM. From Fig.14 to Fig. 16 displays the prototyped flexible PCB for an electric source transmission, the prototyped mechanical system, and the prototyped whole system of the 8.5[mm] outer diameter RUSM.

Fig.12. Prototyped vibrator of the 9[mm] outer diameter RUSM.

(a) Number of teeth is 12

(b) Number of teeth is 14

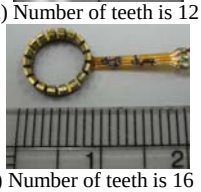

(c) Number of teeth is 16

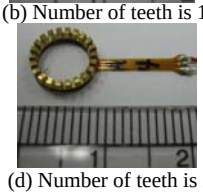

(d) Number of teeth is 22

Fig.13. Prototyped vibrators.

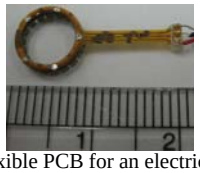

Fig.14. Prototyped flexible PCB for an electric source transmission.

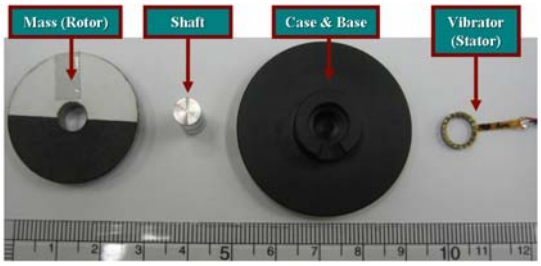

(a) Disassembled mechanical system of the 8.5 [mm] outer diameter RUSM

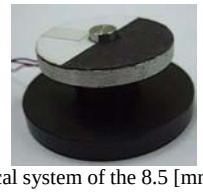

(a) Assembled mechanical system of the 8.5 [mm] outer diameter RUSM

Fig.15. Prototyped mechanical system of the proposed RUSM

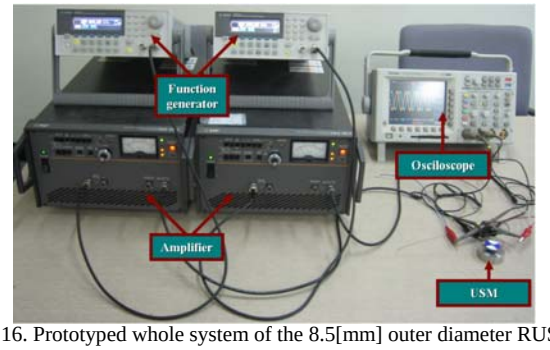

Fig.16. Prototyped whole system of the 8.5[mm] outer diameter RUSM

4 Conclusion

It is remarkable that the exact and efficient analysis and design, with considering complex contact mechanisms, of RUSM is possible with the methodology proposed in this research. This is because the analysis and design method of USM was only using rough analytic methods or using commercial analysis tools or using the trial and error methods. Therefore, it is important to note that the exact and efficient analysis and design of many other kinds of machines, which use similar mechanism, is possible with the suggested methodology.

References:

[1] S. Ueha, Y. Tomikawa, M. Kurosawa, and N. Nakamura, "Ultrasonic Motors: Theory and Applications," Clarendon Press. Oxford, 1993.

[2] Toshiiku Sashida and Takashi Kenjo, "An Introduction to Ultrasonic Motors," Clarendon Press, Oxford, 1993.

[3] Kawasaki, T.Nishikura, M.Sumihara, T.Ohtsuchi, K.Takeda, T.Nojima, and K,Imada, "A small Size Ultrasonic Motor,", *Conference Proceedings, International Conference on Systems Engineering in the Service of Humans*, vol.1 pp.435 – 440, 17-20 Oct., 1993.

[4] K. Uchino, "Piezoelectric Actuator and Ultrasonic Motrs," Kluwer Academic Publishers, 1997.

[5] K. Uchino, and Jayne R. Giniwicz, "Micromechatronics," Marcel Dekker, Inc. New York/Basel, 2002, ch.6.

[6] Koc B., Bouchilloux P., Uchino K., "Piezoelectric micromotor using a metal-ceramic composite structure," *Ultrasonics, Ferroelectrics and Frequency Control, IEEE Transactions*, Vol.47, Issue 4, July 2000 Page(s):836 – 843

[7] Chang-Hwan Lee, Suk-Hee Lee, Hyun-Kyo Jung, Jung-Kun Lee, and Kug-Sun Hong, "Analytic and numerical approaches for characteristic analysis of linear ultrasonic motor," in *Electric Machines and Drives,International Conference IEMD '99*,pp. 619-621, 1999.

[8] Jong-Seok Rho, Byung-Jai Kim, Chang-Hwan Lee, Hyun-Woo Joo and Hyun-Kyo Jung, "Design and Characteristic Analysis of L1B4 Ultrasonic Motor Considering Contact Mechanism," *IEEE Transactions on Ultrasonics, Ferroelectrics and Frequency Control*, Vol.52, pp.2054–2064, 11 Nov. 2005.